Thin Solid Films xxx (2010) xxx–xxx

Contents lists available at ScienceDirect

Thin Solid Films

journal homepage: www.elsevier.com/locate/tsf

Void-free strong bonding of surface activated silicon wafers from room temperature to annealing at 600 °C

M.M.R. Howlader *, F. Zhang

Department of Electrical and Computer Engineering, McMaster University, 1280 Main Street West, Hamilton, ON, Canada L8S 4K1

ARTICLE INFO

Article history:
Received 23 April 2010
Received in revised form 20 August 2010
Accepted 27 August 2010
Available online xxxx

Keywords:
Surface activation
Room temperature bonding
Annealing induced voids
Surface and interface
Bonding strength
Electrical properties
Thermal oxidation
Interfacial amorphous layer

ABSTRACT

In order to investigate the high temperature application of surface activated silicon/silicon wafer bonding, the wafers were bonded at room temperature and annealed up to 600 °C followed by optical, electrical, mechanical and nanostructure characterization of the interface. Void-free interface with high bonding strength was observed that was independent of the annealing temperature. The bonding strength was as high as 20 MPa. The normalized interfacial current density was increased with the increase in the annealing temperature. A thin interfacial amorphous layer with a thickness of 8.3 nm was found before annealing, which was diminished at 600 °C. A correlation between the current density and nanostructure of the interface was observed as a function of the annealing temperature. The high quality silicon/silicon bonding indicates its potential use not only in low temperature microelectronic applications, but also in high temperature harsh environments.

© 2010 Elsevier B.V. All rights reserved.

1. Introduction

Surface activated bonding (SAB) directly joins smooth surfaces after activation using either an argon fast atom beam (Ar-FAB), or an Ar ion beam in an ultrahigh vacuum (UHV) [1–4] at room temperature (RT). The surface activation removes native oxides (i.e., SiO_2 in the case of silicon), carbon contaminants, and makes a smooth surface. The activated smooth surfaces reduce air trapping at the interface, which is one of the causes of void formation. Therefore, the SAB results in a void-free bonded interface that demonstrates high strength without annealing due to spontaneous adhesion between the surfaces.

In contrast to the SAB, hydrophilic Si–O–Si and hydrophobic Si–Si covalent bonding methods require moderate (i.e., 400 °C) and high (i.e., 1100 °C) temperature annealing, respectively to achieve strong bonding required for high temperature environmental applications [5]. However, high temperature annealing is not amenable for materials with different coefficients of thermal expansion, and for prefabricated low melting point metallic layers and polymers [6,7]. In order to avoid these adverse effects, plasma activated bonding (PAB) at an annealing temperature of as low as 200 °C for several days has been reported [6,8]. Although this results in high bonding strength, the interfacial voids remained after the annealing [8,9]. The voids are due to the reactions between the hydroxyl molecule terminated native silicon oxide surfaces in the hydrophilic and PAB, as well as hydrogen terminated silicon surfaces in the hydrophobic bonding at atmospheric pressure.

To address these issues, diverse wafers have been bonded using SAB and the interfaces comprehensively investigated for low temperature optoelectronic, micro-electromechanical systems (MEMS), and microfluidic applications [1–4,7,10]. In fact, Si-based MEMS devices have increased applications in high temperature environments such as the fuel combustion chamber of automotive vehicles (i.e., 450 °C) [11] and the emerging micro gas turbine engine (i.e., 1500 °C) [12]. Under such environments, the bonded interface needs to be robust with optical, electrical, mechanical and structural stabilities that have not been investigated yet in the SAB. This article investigates the annealing influence on the SAB Si/Si interface from room temperature to annealing at 600 °C.

2. Experimental details

Commercially available one-side polished 2-in. (50 mm) silicon (Si) (100) wafers were used. The thicknesses of the wafers were 275 ± 25 µm. The wafers were *p*-type and the resistivity was 1–20 Ω cm.

* Corresponding author.
E-mail address: mrhowlader@ece.mcmaster.ca (M.M.R. Howlader).

0040-6090/$ – see front matter © 2010 Elsevier B.V. All rights reserved.
doi:10.1016/j.tsf.2010.08.144

ARTICLE IN PRESS

The as-received (without pre-treatment) Si surfaces (with ~1–2 nm native oxides) were activated by a 1.5 keV Ar-FAB with 48 mA for 300 s followed by bonding in a UHV pressure of 10^{-7} Pa of a bonding chamber. During activation, the vacuum pressure was 4.2×10^{-2} Pa. The activation sources were placed at 45° with respect to the center of the specimens. The beam activates the surfaces homogeneously throughout the 50 mm diameter wafer.

The bonded specimen was annealed at 200, 400, and 600 °C, respectively for 1 h in each temperature step and then cooled down to RT after each step to characterize the interface through current–voltage (*I–V*) measurements, infrared (IR) camera, tensile pulling and high-resolution transmission microscopy (HRTEM) techniques. For the tensile pulling test and *I–V* measurements, the bonded wafer was cut into 10 mm × 10 mm chips. For *I–V* measurements, the electrodes of 2 mm diameter were made with conductive silver paste at the center on the top and bottom of the bonded specimen before and after annealing.

3. Results and discussion

Fig. 1 shows the IR images of Si/Si wafer bonded interfaces (a) without annealing and after annealing at (b) 200 °C (c) 400 °C and (d) 600 °C. The white areas at the edges of the bonded wafers are due to the blade test. A void-free bonded interface was achieved. The wafers were spontaneously bonded and thermal induced voids were not observed. This behaviour can be explained using the elastic contact theory [13] and molecular dynamics (MD) simulation [14]. In the elastic theory, smooth surface results in a short-range atomic adhesion between the activated surfaces in contact, which has been supported by MD simulations. The MD simulations have predicted covalent bonding between the clean and smooth Si surfaces in UHV at room temperature [14,15]. A smooth surface was confirmed after the surface activation using an atomic force microscope which quantified the surface roughness before and after the surface activation at 0.18 nm and 0.11 nm, respectively.

The void-free interface observed in SAB is in contrast with that in the hydrophilic bonding [8,9,16] and sequentially plasma activated bonding (SPAB) [5,17]. In these methods, a significant number of thermal induced voids were observed due to the interfacial H_2O and H_2 produced from the reaction between OH^- terminated Si wafers after annealing. This is consistent to the simulated results of wafer bonding in which the inclusion of adsorbents on the surfaces strongly affects the bonding properties [14,15]. The OH^- groups not only influence the interfacial voids but also the bonding strength, which will be discussed later. Contrastingly in SAB, the surfaces were activated by Ar-FAB in UHV and hence the OH^- groups were not present on the Si surfaces. Therefore, no reaction by-products were present at the interface and thus no voids were produced after annealing.

Bonding strength is one of the parameters that measure the mechanical stability of an interface. Fig. 2 shows the (a) bonding strength of Si/Si in the SAB, SPAB and hydrophilic bonding, and (b) fracture images of Si/Si interface after tensile pulling for the bonded specimen (i) without annealing and (ii) with annealing at 600 °C. The bonding strength in SAB without annealing was as high as 18 MPa, which was higher than that in the SPAB (~15.5 MPa) [5] and hydrophilic (~0.5 MPa) bonding [18]. The bonding strength in SAB was nearly constant at different annealing temperatures. Note the blade test of Si/Si bonded interface in the SAB failed because of high bonding strength. In contrast, the bonding strength in SPAB remarkably decreased after annealing over 300 °C due to the generation of thermal induced voids at the interface [17]. In hydrophilic bonding, the bonding strength was increased with the annealing temperature due to the shrinkage of chains of OH^- molecules [17]. Even after annealing at 1100 °C, it was lower than that in the SAB without annealing. The high bonding strength in the SAB resulted in bulk fracture in Si but not interfacial delamination at

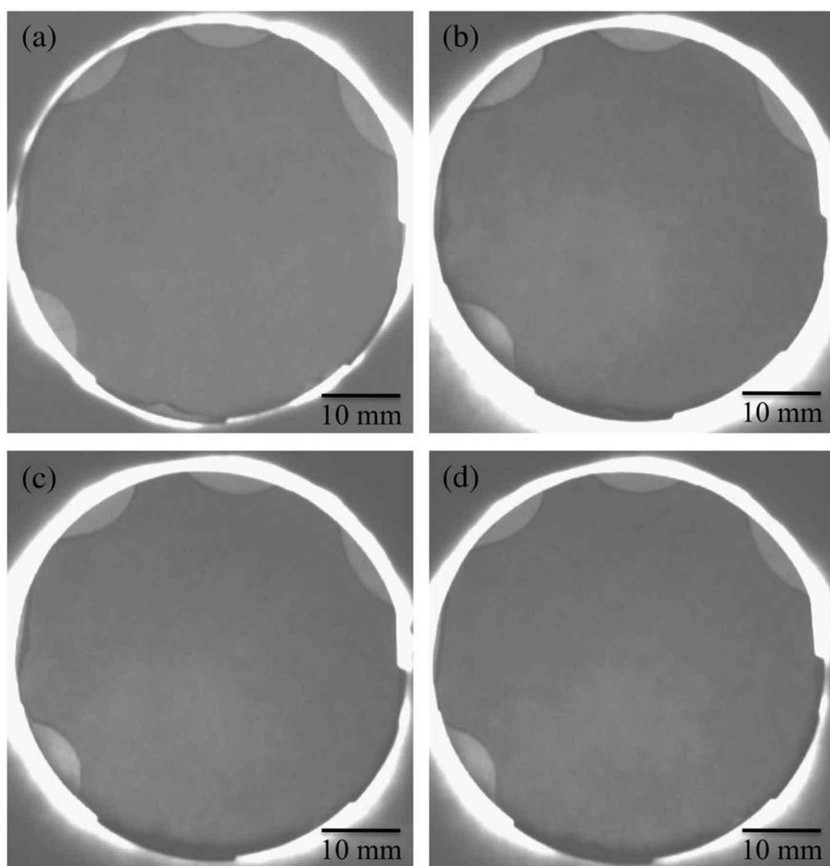

Fig. 1. Infrared (IR) transmission images of bonded Si/Si wafers in SAB (a) without annealing and after annealing at (b) 200 °C (c) 400 °C and (d) 600 °C.

Please cite this article as: M.M.R. Howlader, F. Zhang, Thin Solid Films (2010), doi:10.1016/j.tsf.2010.08.144

ARTICLE IN PRESS

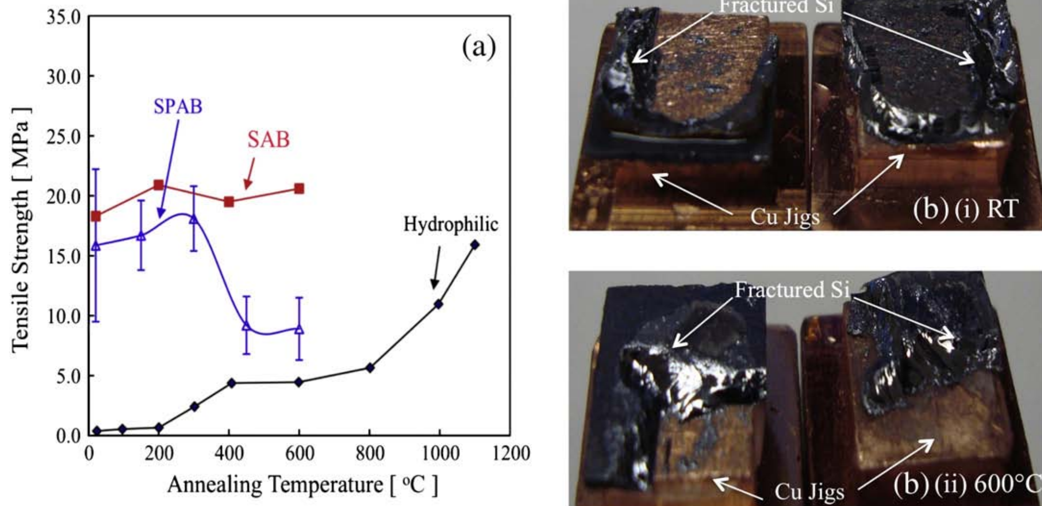

Fig. 2. (a) Bonding strength as a function of annealing temperature in SAB, SPAB and hydrophilic bonding. (b) Fracture images of the Si wafers after tensile pulling (i) before annealing and (ii) after annealing at 600 °C.

both RT and 600 °C (annealed for 1 h) (Fig. 2b). After the tensile pulling test, fractured Si remained on Cu jigs on both sides, as shown in Fig. 2(b). This high bonding strength is attributed to the covalent bonding between the atoms of the cleaned and smooth mated surfaces.

The influence of annealing on the current transport properties of the bonded interface was investigated using *I–V* measurements. Fig. 3(a) shows the *I–V* characteristics of *p–p* Si bonded interfaces before and after normalization of the current density. Inset shows the *I–V* curves in the magnified form before normalization when the current density of the interface was decreased with the increase of annealing temperatures. Indeed, this was caused by the thermal oxide of the Si surfaces during annealing. In order to avoid the influence of thermal oxides on Si surfaces from the interface current, a single Si wafer was annealed at identical conditions to that of the bonded specimen to measure its *I–V* characteristics. Fig. 3(b) shows the current density of a single Si wafer before and after annealing. The current density of the single Si wafer was decreased with an increase in annealing temperatures due to annealing induced Si oxides. The interface current density was normalized to the current density of the single Si surfaces with thermal oxides. The normalized current can be expressed by the following equation.

$$\sigma_2 = \sigma_1 \times \left(\frac{\sigma_3}{\sigma_4}\right), \quad (1)$$

where σ_1 and σ_2 are the current densities of the interface before and after normalization, σ_3 and σ_4 are the current densities of a single Si wafer before bonding at room temperature and after annealing at different temperatures that includes the current due to thermal oxides of the Si surfaces (Fig. 3b).

After normalization, the electrical current density was increased with the annealing temperature (Fig. 3a) due to the exclusion of thermal oxides of the Si surfaces, and morphological changes at the interface. Also, this increase was attributed to the annihilation of radiation induced interfacial defects and recombination centers [7]. The morphological relationship with the increase in the current density can be explained through the investigation of nanostructure behaviour through HRTEM.

Fig. 4 shows the HRTEM images of Si/Si bonded interface before and after annealing at 200 °C, 400 °C and 600 °C. No interfacial voids or fractures at the nanometer scale were found from these images. Before annealing, an interfacial amorphous layer with a thickness of 8.3 nm was observed. This result is consistent with that of the previous study [4]. The interfacial amorphous layer is attributed to Ar ion induced surface damage during activation [4,7]. Despite the presence of an amorphous layer at the bonded interface, high bonding strength was achieved before and after annealing. Therefore, the amorphous layer provides extended bonding flexibility in diverse crystallographic-oriented wafers. After annealing, the amorphous

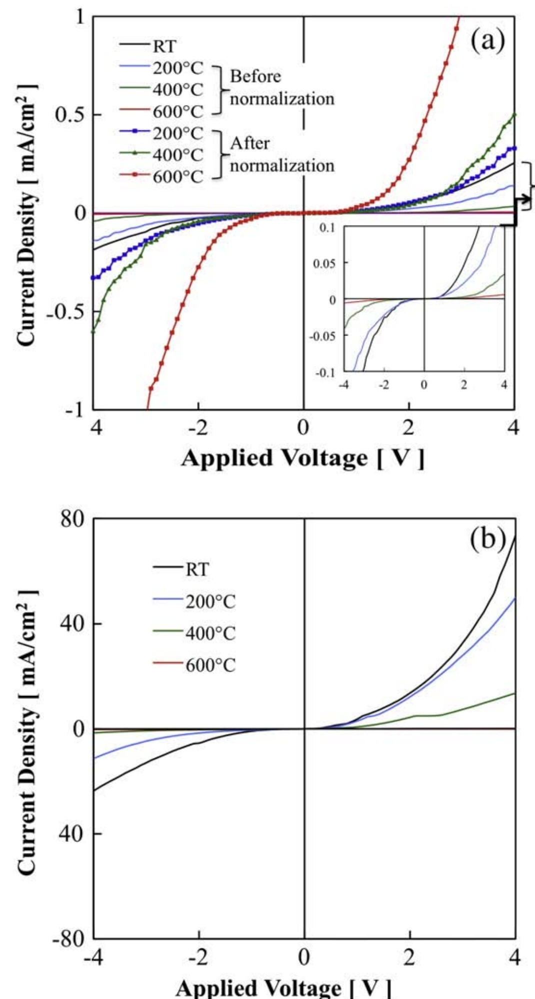

Fig. 3. (a) Current–voltage (*I–V*) characteristics of the bonded interface as a function the annealing temperature with and without normalization. (b) Current density of a single Si wafer before (RT) and after annealing at different temperatures.

Please cite this article as: M.M.R. Howlader, F. Zhang, Thin Solid Films (2010), doi:10.1016/j.tsf.2010.08.144

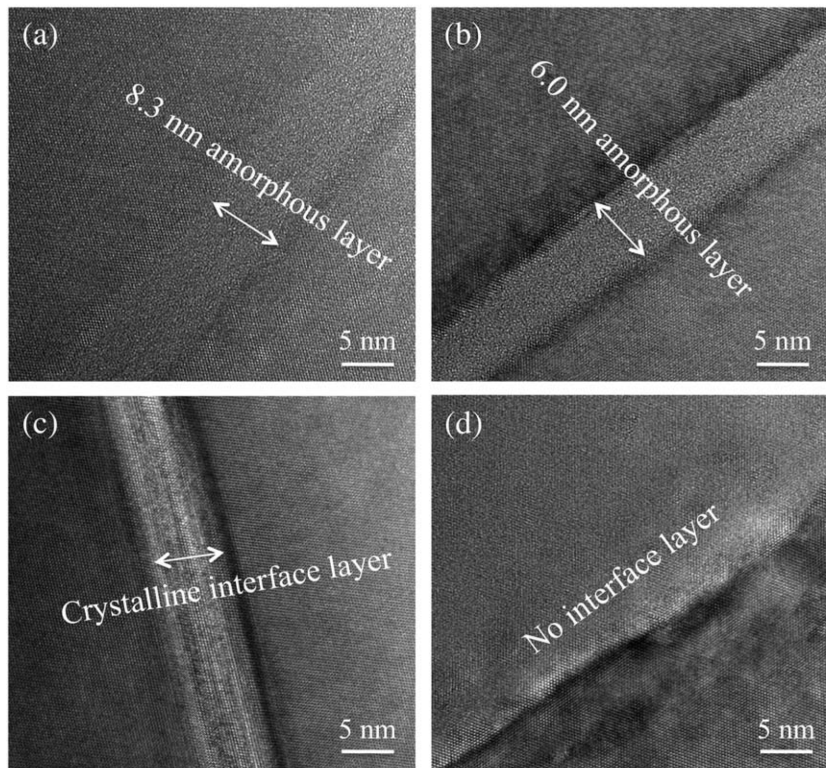

Fig. 4. Nano-interface of Si/Si (a) before annealing and after annealing at (b) 200 °C, (c) 400 °C and (d) 600 °C. The amorphous layer before annealing decreases as the temperature increases and disappears at 600 °C.

layer was first decreased to 6.0 nm at 200 °C, then changed to crystalline layer of 6.0 nm thick at 400 °C, and finally diminished at 600 °C. The decrease in the interfacial amorphous layers increased the current density as shown in Fig. 4(a) and it is consistent with that of GaAs/GaP as reported in [7].

In harsh environments, the bonded interface is not only exposed to high temperatures, but also to chemicals and high pressure. The bonding strength of Si/Si interface in the SAB was better than that in the SPAB after dipping in 3% hydrofluoric acid, acetone and ethanol [19]. This is again due to the bonding between the clean surfaces free-from absorbents and oxides. The effect of high pressure (HP) and high temperature (HT) treatment has been investigated on Si on insulator (SOI) structures [20]. The HP and HT induced hydrogen and oxygen diffusion have been observed. Such diffusion and interfacial voids are absent in the SAB. The HP effect on the bonding strength of Si/Si is under investigation. In summary, the Si/Si bonded wafers in the SAB can be applied for MEMS devices in high temperature harsh environments [12,21] because of void-free robust interface.

4. Conclusions

Annealing temperature independent void-free Si/Si interface with high bonding strength at 20 MPa was observed up to 600 °C. The normalized interfacial current density was increased with annealing temperatures, which was attributed to the thermal annihilation of the radiation induced interfacial defects and recombination centers due to annealing. A thin interfacial amorphous layer with a thickness of 8.3 nm was found before annealing, which was diminished at 600 °C. A correlation between the current density and amorphous layer of the interface was observed as a function of the annealing temperature. Therefore, the SAB processed Si/Si bonding has a potential use not only in low temperature microelectronics, but also in high temperature harsh environments.

Acknowledgement

This research is supported by a discovery grant (No. 327947) from the Natural Science and Engineering Research Council of Canada and an infrastructure grant (No. 12128) from the Canada Foundation for Innovation (CFI). Professor Jamal Deen is greatly appreciated for his support and assistance in establishing nano-bonding and interconnection research at the Micro- and Nano-Systems Laboratory at McMaster University. The authors acknowledge Professor Tadatomo Suga of The University of Tokyo and A. Yamauchi of Bondtech Corporation, Japan for the construction of the Nano-bonding and interconnect system (NBIS) equipment. M. G. Kibria of McMaster University is appreciated for his assistance in writing the manuscript, and the Canada Center for Electron Microscopy (CCEM) at McMaster University is acknowledged for the assistance in the HRTEM experiments.

References

[1] H. Takagi, K. Kikuchi, R. Maeda, T.R. Chung, T. Suga, Appl. Phys. Lett. 68 (1996) 2222.
[2] T. Chung, N. Hosoda, T. Suga, H. Takagi, Appl. Phys. Lett. 72 (1998) 1565.
[3] M.M.R. Howlader, T. Suga, M.J. Kim, Appl. Phys. Lett. 89 (2006) 031914.
[4] H. Takagi, R. Maeda, N. Hosoda, T. Suga, Jpn. J. Appl. Phys. 1 38 (1999) 1589.
[5] M.M.R. Howlader, T. Suga, H. Itoh, T.H. Lee, M.J. Kim, J. Electrochem. Soc. 156 (2009) H846.
[6] T. Suni, K. Henttinen, I. Suni, J. Makinen, J. Electrochem. Soc. 149 (2002) G348.
[7] M.M.R. Howlader, T. Suga, F. Zhang, T.H. Lee, M.J. Kim, Electrochem. Solid State Lett. 13 (2010) H61.
[8] T.L. Alford, T. Tang, D.C. Thompson, S. Bhagat, J.W. Mayer, Thin Solid Films 516 (2008) 2158.
[9] U. Gösele, Q.-Y. Tong, Annu. Rev. Mater. Sci. 28 (1998) 215.
[10] M.M.R. Howlader, H. Okada, T.H. Kim, T. Itoh, T. Suga, J. Electrochem. Soc. 151 (2004) G461.
[11] S. Kruger and W. Gessner, Springer-Verlag Berlin Heideberg New York, p.253.
[12] C.M. Spadaccini, A. Mehra, J. Lee, X. Zhang, S. Lukachko, I.A. Waitz, J. Eng. Gas Turbines Power 125 (2003) 709.
[13] C. Gui, M. Elwenspoek, N. Tas, J.G.E. Gardeniers, J. Appl. Phys. 85 (1999) 7448.
[14] D. Conrad, K. Scheerschmidt, U. Gosele, Appl. Phys. A 62 (1996) 7.

ARTICLE IN PRESS

[15] U. Gosele, H. Stenzel, T. Martini, J. Steinkirchner, D. Conrad, K. Scheerschmidt, Appl. Phys. Lett. 67 (1995) 3614.
[16] X. Zhang, J.-P. Raskin, Electrochem. Solid State Lett. 8 (2004) G172.
[17] M.M.R. Howlader, F. Zhang, M.G. Kibria, J. Micromech. Microeng. 20 (2010) 065012.
[18] M. Shimbo, K. Furukawa, K. Fukuda, K. Tanzawa, J. Appl. Phys. 60 (1986) 2987.
[19] M.M.R. Howlader, S. Suehara, H. Takagi, T.H. Kim, R. Maeda, T. Suga, IEEE Trans. Adv. Packag. 29 (2006) 448.
[20] A. Misiuk, L. Bryja, J. Bak-Misiuk, J. Ratajczak, I.V. Antonova, V.P. Popov, Cryst. Eng. 5 (2002) 155.
[21] M. Esashi, J. Micromech. Microeng. 18 (2008) 073001.

Please cite this article as: M.M.R. Howlader, F. Zhang, Thin Solid Films (2010), doi:10.1016/j.tsf.2010.08.144